1 # Underestimation of brown carbon absorption based on the

2 # methanol extraction method and its impacts on source analysis

3

4 Zhenqi Xu[a], Wei Feng[a], Yicheng Wang[a], Haoran Ye[a], Yuhang Wang[b], Hong Liao[a],

5 Mingjie Xie[a,*]

6

7 [a]Collaborative Innovation Center of Atmospheric Environment and Equipment

8 Technology, Jiangsu Key Laboratory of Atmospheric Environment Monitoring and

9 Pollution Control, School of Environmental Science and Engineering, Nanjing

10 University of Information Science & Technology, 219 Ningliu Road, Nanjing 210044,

11 China

12 [b]School of Earth and Atmospheric Sciences, Georgia Institute of Technology, Atlanta,

13 GA 30332, United States

14

15 *Corresponding to:

16 Mingjie Xie (mingjie.xie@nuist.edu.cn, mingjie.xie@colorado.edu);

17 Mailing address: 219 Ningliu Road, Nanjing, Jiangsu, 210044, China

18

19

20

21

22

23

24

25

26

27

28 **Abstract**

29   The methanol extraction method was widely applied to isolate organic carbon (OC)

30 from ambient aerosols, followed by measurements of brown carbon (BrC) absorption.

31 However, undissolved OC fractions will lead to underestimated BrC absorption. In this

32 work, water, methanol (MeOH), MeOH/dichloromethane (MeOH/DCM, 1:1, v/v),

33 MeOH/DCM (1:2, v/v), tetrahydrofuran (THF), and N,N-dimethylformamide (DMF)

34 were tested for extraction efficiencies of ambient OC, and the light absorption of

35 individual solvent extracts was determined. Among the five solvents and solvent

36 mixtures, DMF dissolved the highest fractions of ambient OC (up to ~95%), followed

37 by MeOH and MeOH/DCM mixtures (< 90%), and the DMF extracts had significant

38 ($p < 0.05$) higher light absorption than other solvent extracts. This is because the OC

39 fractions evaporating at higher temperatures (> 280°C) are less soluble in MeOH (~80%)

40 than in DMF (~90%) and contain stronger light-absorbing chromophores. Moreover,

41 the light absorption of DMF and MeOH extracts of collocated aerosol samples in

42 Nanjing showed distinct time series. Source apportionment results indicated that the

43 MeOH insoluble OC mainly came from unburned fossil fuels and polymerization

44 processes of aerosol organics. These results highlight the necessity of replacing MeOH

45 with DMF for further investigations on structures and light absorption of low-volatile

46 BrC.

47

48

49

50

51

52

Atmospheric
Chemistry
and Physics
Discussions

Open Access

EGU

1 Introduction

53

54   Besides black carbon (BC) and mineral dust, growing evidence shows that organic

55 carbon (OC) aerosols derived from various combustion sources (e.g., biofuel and fossil

56 fuel) and secondary processes (e.g., gas-phase oxidation, aqueous and in-cloud

57 processes) can absorb sunlight at short visible and UV wavelengths (Laskin et al., 2015;

58 Hems et al., 2021). The radiative forcing (RF) of the light-absorbing organic carbon,

59 also termed "brown carbon" (BrC), is not well quantified due to the lack of its emission

60 data and large uncertainties in *in situ* BrC measurements (Wang et al., 2014; Wang et

61 al., 2018; Saleh, 2020). The imaginary part of the refractive index (k) of BrC is required

62 when modeling its influence on aerosols direct RF, and is retrieved by the optical

63 closure method combing online monitoring of aerosol absorption and size distributions

64 with Mie theory calculations (Lack et al., 2012; Saleh et al., 2013; Saleh et al., 2014).

65 However, several pre-assumptions must be made on aerosol morphology (spherical Mie

66 model) and mixing states of BC and organic aerosols (OA), which might introduce large

67 uncertainties in the estimation of k (Mack et al., 2010; Xu et al., 2021).

68   To improve the understanding on chemical composition and light-absorbing

69 properties of BrC chromophores, organic matter (OM) in aerosols was isolated through

70 solvent extraction using water and/or methanol, followed by filtration and a series of

71 instrumental analysis (e.g., UV/Vis spectrometer, liquid chromatograph-mass

72 spectrometer; Chen and Bond, 2010; Liu et al., 2013; Lin et al., 2016). Referring to

73 existing studies, a larger fraction of the methanol extract absorption comes from water-

74 insoluble OM containing conjugated structures (Chen and Bond, 2010; Huang et al.,

75 2020); the light absorption of biomass burning OM is majorly contributed by large

76 molecules (MW > 500~1000 Da; Di Lorenzo and Young, 2016; Di Lorenzo et al., 2017)

77 and depends on burn conditions (Saleh et al., 2014); polycyclic aromatic hydrocarbons

Atmospheric
Chemistry
and Physics
Discussions

78   (PAHs) and nitroaromatic compounds (NACs) are ubiquitous BrC chromophores in the

79   atmosphere (Huang et al., 2018; Wang et al., 2019), but the identified species only

80   explain a few percentages (< 10%) of total BrC absorption (Huang et al., 2018; Li et

81   al., 2020).

82   Methanol can extract > 90% OM from biomass burning (Chen and Bond, 2010;

83   Xie et al., 2017b), while the extraction efficiency (η, %) decreases to ~80% for ambient

84   organic aerosols (Xie et al., 2019b; Xie et al., 2022) possibly due to other sources

85   emitting large hydrophobic molecules and oligomerizations of small molecules during

86   the aging process (Cheng et al., 2021; Li et al., 2021). The light-absorbing properties

87   and structures of methanol-insoluble OC (MIOC) are still unknown. By comparing BrC

88   characterization results of offline and online methods, some studies conclude that the

89   MIOC dominates BrC absorption in source and ambient aerosols (Bai et al., 2020; Atwi

90   et al., 2022). However, the online-retrieval and offline-extraction methods are designed

91   based on different instrumentation and purposes, and the online method depends largely

92   on presumed and uncertain optical properties of BC (Wang et al., 2014). Thus, BrC

93   absorption in particles and solution can hardly be compared directly. To reveal the

94   absorption and composition of MIOC, it is necessary to find a new solvent or develop

95   a new methodology to improve OC extraction efficiency (Shetty et al., 2019).

96   In this work, a series of single solvents and solvent blends were tested for extraction

97   efficiencies of OC in ambient particulate matter with aerodynamic diameter < 2.5 μm

98   ($PM_{2.5}$), and the sample extract absorption of each solvent was compared. The solvent

99   or solvent mixture with the highest η value was applied to extract a matrix of collocated

100   $PM_{2.5}$ samples followed by light absorption measurements. In our previous work, the

101   light absorption of methanol extracts of the same samples was measured, and source

102   apportionment was performed using organic molecular marker data (Xie et al., 2022).

103 By comparing with the study results in Xie et al. (2022), this study evaluated the

104 underestimation of BrC absorption in methanol and its impacts on BrC source

105 attributions. These results suggest that methanol should be replaced in future solvent

106 extraction-based investigations on the absorption, composition, sources, and formation

107 pathways of low-volatile BrC.

108 **2. Methods**

109 *2.1 Solvent selection*

110 Five solvents and solvent mixtures including water, methanol (MeOH),

111 MeOH/dichloromethane (MeOH/DCM, 1:1, v:v), MeOH/DCM (1:2, v:v),

112 tetrahydrofuran (THF), and N,N-dimethylformamide (DMF) were selected to extract

113 OC from identical $PM_{2.5}$ samples to determine which solvent or solvent mixture has the

114 highest η value. Water and methanol are the most commonly used solvents to extract

115 BrC from source or ambient particles. Cheng et al. (2021) found that OC produced

116 through the combustion of toluene, isooctane, and cyclohexane were more soluble in

117 DCM than MeOH. Since a major part of BrC absorption is coming from unknown large

118 molecules (Di Lorenzo and Young, 2016; Di Lorenzo et al., 2017), polar aprotic

119 solvents THF and DMF were tested due to their high capacity for dissolving large

120 polymers. Except for water and MeOH, MeOH/DCM mixtures, THF, and DMF were

121 rarely used to extract OC for light absorption measurements.

122 *2.2 Sampling*

123 **Sampling for solvent test.** To compare OC extraction efficiencies and extract

124 absorption of the five selected solvents and solvent mixtures, twenty-one ambient $PM_{2.5}$

125 samples were collected on the rooftop of a seven-story library building in Nanjing

126 University of Information Science and Technology (NUIST, 32.21ºN, 118.71ºE).

127 Details of the sampling site and equipment were provided by Yang et al. (2021). Two

Atmospheric
Chemistry
and Physics
Discussions

128   identical mid-volume samplers (Sampler I and II; $PM_{2.5}$-PUF-300, Mingye

129   Environmental, China) equipped with 2.5 μm cut-point impactors were used for

130   ambient air sampling during day-time (8:00 a.m.–7:00 p.m.) and night-time (8:00 p.m.–

131   7:00 a.m. the next day), respectively, in December 2019. After the impactor, $PM_{2.5}$ in

132   the air stream was collected on a pre-baked (550 °C, 4 h) quartz filter (20.3 cm ×12.6

133   cm, Munktell Filter AB, Sweden) at a flow rate of 300 L min^{-1}. $PM_{2.5}$ filter and field

134   blank samples were sealed and stored at –20 °C before chemical analysis. Information

135   about $PM_{2.5}$ samples for the solvent test is provided in Table S1 of supplementary

136   information.

137   **Ambient sampling for BrC analysis.** Details of the ambient sampling were described

138   in previous work (Qin et al., 2021; Yang et al., 2021; Xie et al., 2022). Briefly, Sampler

139   I and II were equipped with two quartz filters in series (quartz behind quartz, QBQ

140   method; Q_f and Q_b) followed by adsorbents. Collocated filter and adsorbent samples

141   were collected every sixth day during daytime and nighttime from 2018/09/28 to

142   2019/09/28. Field blank sampling was performed every 10th sample to address

143   contamination. Q_f samples loaded with $PM_{2.5}$ were speciated and extracted for light

144   absorption measurements. The OC adsorbed on Q_b and its light absorption were

145   analyzed to determine positive sampling artifacts. The adsorbents in sampler I [a

146   polyurethane foam (PUF)/XAD-4 resin/PUF sandwich] and II (a PUF plug) were used

147   to collect gas-phase nonpolar and polar organic compounds, respectively.

148   *2.3 Solvent test for light absorption and extraction efficiency*

149   An aliquot (~6 cm^2) of each filter sample was extracted ultrasonically in 10 mL of

150   each solvent or solvent mixture (HPLC grade) for 30 min (one-time extraction

151   procedure, $N = 11$; Table S1). After filtration, the light absorbance (A_λ) of individual

152   solvent extracts was measured over 200–900 nm using a UV/Vis spectrometer (UV-

153   1900, Shimadzu Corporation, Japan), and was converted to light absorption coefficient

154   (Abs_λ, Mm^{-1}) by

155    $$Abs_\lambda = (A_\lambda - A_{700}) \times \frac{V_l}{V_a \times L} \ln(10) \qquad (1)$$

156   where A_{700} is subtracted to correct baseline drift, V_l (m^3) is the air volume of the

157   extracted sample, L (0.01 m) is the optical path length, and ln (10) was multiplied to

158   transform Abs_λ from a common to a natural logarithm (Hecobian et al., 2010). To

159   understand if multiple extractions could draw out more BrC, a two-time extraction

160   procedure was applied for another 10 ambient $PM_{2.5}$ samples in the same manner (Table

161   S1). The A_λ of the 1st and 2nd extractions (10 mL each) was measured separately for

162   Abs_λ calculations.

163   Prior to solvent extractions, the concentrations of OC and EC in each filter sample

164   were analyzed using a thermal-optical carbon analyzer (DRI, 2001A, Atmoslytic,

165   United States) following the IMPROVE-A protocol. OC and EC were converted to CO_2

166   step by step during two separate heating cycles [OC1 (140°C) – OC2 (280°C) – OC3

167   (480°C) – OC4 (580°C) in pure He, EC1 (580°C) – EC2 (740°C) – EC3 (840°C) in 98%

168   He/2% O_2], and the emitted CO_2 during each heating step was converted to CH_4 and

169   measured using a flame ionization detector (FID).

170   After extractions, filters extracted by MeOH, MeOH/DCM (1:1), MeOH/DCM

171   (1:2), and THF were air-dried in a fume hood and analyzed for residual OC (rOC, μg

172   m^{-3}) using the identical method. Filters extracted in water and DMF cannot be air-dried

173   in the short term due to the low volatility of solvents, and their rOC was measured after

174   baking at 100 °C for 2 h. The total amount of OC dissolved in water for each sample

175   was also measured as water-soluble OC (WSOC) by a total organic carbon analyzer

176   (TOC-L, Shimadzu, Japan; Yang et al., 2021). To examine if the baking process would

177   influence rOC measurements, the rOC of filters extracted in MeOH, MeOH/DCM

178   mixtures, and THF were also measured after the baking process and compared to those

179   determined after air dried. The pyrolytic carbon (PC) was used to correct for sample

180   charring and was determined when the filter transmittance or reflectance returned to its

181   initial value during the analysis (Schauer et al., 2003), but the formation of PC is very

182   scarce when analyzing extracted filters. In this study, solvent-extractable OC (SEOC,

183   μg m^{-3}) was determined by the difference in OC1–OC4 between pre- and post-

184   extraction samples. The extraction efficiency (η, %) of each solvent was expressed as

185    $$\eta = \frac{\text{SEOC}}{\text{OC}} \times 100\% \qquad (2)$$

186   Here, SEOC denotes WSOC when the solvent is water. For the ambient samples

187   extracted twice, rOC was measured only after the two-extraction procedure was

188   completed.

189   The solution mass absorption efficiency (MAE$_\lambda$, m^2 g^{-1} C) was calculated by

190   dividing Abs$_\lambda$ by the concentration of SEOC

191    $$\text{MAE}_\lambda = \frac{\text{Abs}_\lambda}{\text{SEOC}} \qquad (3)$$

192   and the solution absorption Ångström exponent (Å), a parameter showing the

193   wavelength dependence of solvent extract absorption, was obtained from the regression

194   slope of lg (Abs$_\lambda$) versus lg (λ) over 300–550 nm.

195   To evaluate the influence of solvent effects on light absorption of different solvent

196   extracts of the same sample, solutions of 4-nitrophenol at 1.90 mg L^{-1}, 4-nitrocatechol

197   at 1.84 mg L^{-1}, and 25-PAH mixtures (Table S2) at 0.0080 mg L^{-1} and 0.024 mg L^{-1}

198   (each species) in the five solvents and solvent mixtures were made up for five times

199   and analyzed for UV/Vis spectra. The absorbance of PAH mixtures in water was not

200   provided due to their low solubility.

201   *2.3 Measurements and analysis of ambient BrC absorption*

202   Collocated Q_f and Q_b samples were extracted using the solvent with the highest η

203   value once followed by light absorbance measurement. OC concentrations in Q_f and Q_b

204   samples were obtained from Yang et al. (2021), and SEOC values were estimated from

205   OC concentrations and the average η value determined in *section 2.1* for one-time

206   extraction. In this work, Q_b measurements were used to correct Abs_λ, MAE_λ, and Å of

207   BrC in ambient PM$_{2.5}$ in the same manner as those for water and methanol extracts in

208   Xie et al. (2022)

209   Artifact-corrected $Abs_\lambda = Abs_\lambda^{Qf} - Abs_\lambda^{Qb}$ (4)

210   Artifact-corrected $MAE_\lambda = \frac{Abs_\lambda^{Qf} - Abs_\lambda^{Qb}}{SEOC_{Qf} - OC_{Qb}}$ (5)

211   where Abs^{Qf}_λ and Abs^{Qb}_λ are Abs_λ values of Q_f and Q_b samples, respectively; $SEOC_{Qf}$

212   represents SEOC concentrations in Q_f samples; OC_{Qb} denotes OC concentrations in Q_b

213   samples, assuming that OC in Q_b is completely dissolved (Xie et al., 2022). Artifact

214   corrected Å were generated from the regression slope of lg (Abs^{Qf}_λ - Abs^{Qb}_λ) versus lg

215   (λ) over 300 – 550 nm. Artifact-corrected Abs_λ, MAE_λ, and Å during each sampling

216   interval were determined by averaging each pair of collocated measurements. If one of

217   the two numbers in a pair is missed, the other number will be directly used for the

218   specific sampling interval. To compare with previous studies based on water and/or

219   methanol extraction methods, Abs_λ and MAE_λ at 365 nm were shown and discussed in

220   this work.

221   Pearson's correlation coefficient (*r*) was used to show how collocated

222   measurements of BrC in ambient PM$_{2.5}$ vary together. The coefficient of divergence

223   (COD) was calculated to indicate consistency between collocated measurements. The

224   relative uncertainty of BrC absorption derived from duplicate data was depicted using

225   the average relative percent difference (ARPD, %), which was used as the uncertainty

226   fraction for BrC measurements. Calculation methods of COD and ARPD are provided

227   in Text S1 of supplementary information. To examine the influence of BrC

228   underestimation based on the methanol extraction method on source apportionment,

229   positive matrix factorization (PMF) version 5.0 (U.S. Environmental Protection

230   Agency) was applied to attribute the light absorption of aerosol extracts in methanol

231   and solvent with the highest η to sources. The input bulk components and organic

232   molecular marker (OMM) data for PMF analysis were obtained from Xie et al. (2022)

233   and are summarized in Table S3. Four- to ten-factor solutions were tested to retrieve a

234   final factor number with the most physically interpretable base-case solution.

235   **3. Results and discussion**

236   *3.1 Solvent test*

237   3.1.1 Extraction efficiency of different solvents

238   The concentrations of OC and EC fractions in each sample prior to solvent

239   extractions are listed in Table S1. SEOC concentrations and extraction efficiencies of

240   individual solvents and solvent mixtures are detailed in Table 1. Generally, DMF

241   presented the highest extraction efficiency of total OC whenever filter samples were

242   extracted once (89.0 ± 7.96%) or twice (95.6 ± 3.67%), followed by MeOH (one-time

243   extraction 82.3 ± 8.68%, two-time extraction 86.6 ± 7.86%) and MeOH/DCM mixtures

244   (~75%, ~85%). Although THF and DMF are frequently used to dissolve polymers (e.g.,

245   polystyrene) for characterization, THF had the lowest η values (64.2 ± 8.08%, 70.1 ±

246   8.01%) comparable to water (66.7 ± 8.58%, 69.9 ± 5.88%). Compared with one-time

247   extraction, the extraction efficiencies of selected solvents were improved by a few

248   percent when filter samples were extracted twice, and η values of MeOH/DCM

249   mixtures became closer to those of MeOH (Table 1). These results showed that solvents

Atmospheric
Chemistry
and Physics
Discussions

Open Access

EGU

250 can reach more than 80% of their dissolving capacity with the one-time extraction, and

251 the ambient OC in Nanjing is more soluble in MeOH than DCM.

252   From OC1 to OC4, the volatility of OC fractions is expected to decrease

253 continuously, and the molecules in OC fractions evolving at higher temperatures should

254 be larger than those in OC1 with similar functional groups. In Table 1, MeOH and

255 MeOH/DCM mixtures had comparable or even higher η values ($82.6 \pm 25.9\%$–$97.9 \pm$

256 5.02%) of OC1 and OC2 than DMF ($88.8 \pm 4.98\%$–$97.2 \pm 2.12\%$). But OC3 and OC4

257 accounted for more than 60% of OC concentrations, and DMF exhibited significant (p

258 < 0.05) larger η values than other solvents, indicating that DMF had stronger dissolving

259 capacity for large organic molecules than MeOH.

260   Concentrations of extracted OC fractions in MeOH, MeOH/DCM mixtures, and

261 THF based on the two methods for rOC measurements (*section 2.2*) are compared in

262 Figures S1 and S2. The total SEOC concentrations derived from the two methods are

263 compared in Figure S3. All the scatter data of SEOC fell along the 1:1 line with

264 significant correlations ($r > 0.85$, $p < 0.01$). Because the measurement uncertainty of

265 dominant species is lower than minor ones (Hyslop and White, 2008; Yang et al., 2021),

266 the slightly greater relative difference between the two methods for extractable OC1

267 was likely attributed to its low concentrations (< 1 µg m^{-3}; Tables 1 and S1). Thus,

268 baking extracted filters to dryness was expected to have little influence on SEOC

269 measurements, particularly for low-volatile OC fractions (OC2-OC4).

270   Although water dissolves less OC than MeOH, WSOC is intensively extracted and

271 analyzed for its composition and light absorption (Hecobian et al., 2010; Liu et al., 2013;

272 Washenfelder et al., 2015). WSOC can play a significant role in changing the radiative

273 and cloud-nucleating properties of atmospheric aerosols (Hallar et al., 2013; Taylor et

274 al., 2017). It also served as a proxy measurement for oxygenated (OOA) or secondary

Atmospheric
Chemistry
and Physics
Discussions
Open Access
EGU

275   organic aerosols (SOA) in some regions (Kondo et al., 2007; Weber et al., 2007). In

276   previous work, MeOH was commonly used as the most efficient solvent in extracting

277   OC from biomass burning ($\eta > 90\%$; Chen and Bond, 2010; Xie et al., 2017b) and

278   ambient particles ($\eta \sim 80\%$; Xie et al., 2019b; Xie et al., 2022). MeOH-insoluble OC

279   has rarely been investigated through direct solvent-extraction followed by instrumental

280   analysis. There is evidence showing that BrC absorption is associated mostly with large

281   molecular weight and extremely low-volatile species (Saleh et al., 2014; Di Lorenzo

282   and Young, 2016; Di Lorenzo et al., 2017). Compared with DMF, the lower capability

283   of MeOH in dissolving OC3 and OC4 would lead to an underestimation of BrC

284   absorption in atmospheric aerosols.

285   3.1.2 Light absorption of different solvent extracts

286   Table 2 shows the average Abs_λ and MAE_λ values of different solvent extracts at

287   365 and 550 nm. The Abs_λ and MAE_λ spectra of selected samples are illustrated in

288   Figure S4. Not including DMF, MeOH extracts exhibited the strongest light absorption.

289   Since MeOH can dissolve more OC3 and OC4 than DCM (Table 1), the Abs_λ and MAE_λ

290   of MeOH/DCM extracts decreased as the fraction of DCM increased in solvent

291   mixtures (Table 2 and Figure S4). Water and THF extracts had the smallest Abs_λ and

292   MAE_λ due to their low extraction efficiencies for low-volatile OC (OC2-OC4; Table 1).

293   In comparison to MeOH extracts, $Abs_{365/550}$ and $MAE_{365/550}$ of DMF extracts were at

294   least more than 40% higher ($p < 0.05$). Given that the relative difference in extraction

295   efficiency of total OC between MeOH and DMF was less than 10%, low-volatile OC

296   should contain stronger light-absorbing chromophores (Saleh et al., 2014). Moreover,

297   the relative difference in Abs_λ and MAE_λ between MeOH and DMF extracts increased

298   with wavelength (Figure S4). This is because the light absorption of DMF extracts

299   depends less on wavelengths than other solvent extracts (Å ~4.5, Table 2).

300   In this work, insoluble organic particles coming off the filter during sonication

301   might lead to overestimated SEOC concentrations and η values, and then the MAE_λ of

302   solvent extracts would be underestimated. Previous studies rarely considered the loss

303   of insoluble OC during the extraction process (Yan et al., 2020), of which the impact

304   on MAE_λ calculation was still inconclusive. But Abs_λ measurements would never be

305   influenced, as the light absorbance of solvent extracts was analyzed after filtration. In

306   Table 2, the second extraction only increases the average Abs_{365} and Abs_{550} values of

307   DMF extracts by 6.70% ($p = 0.78$) and 6.76% ($p = 0.77$), respectively. We suspected

308   that the difference in η values of DMF between one-time and two-time extraction

309   procedures was mainly ascribed to the detachment of insoluble OC particles.

310   In Figure S5, the UV/Vis spectra of 4-nitrophenol and 4-nitrocatechol in DMF are

311   very different from other solvents with maximum absorbance at ~450 nm, indicating

312   that the solvent type should influence solution absorption. However, the absorbance of

313   4-nitrophenol and 4-nitrocatechol in DMF at 365 nm (A_{365}) was lower than that in

314   MeOH, and PAH solutions showed very similar absorbance spectra across the five

315   solvents (Figure S5g–l and Table S4). Considering that low-volatile OC fractions (e.g.,

316   OC3 and OC4) in the ambient are less water soluble (Table 1) and have a high degree

317   of conjugation (Chen and Bond, 2010; Lin et al., 2014), their structures are probably

318   featured by a PAH skeleton. Therefore, the large difference in Abs_{365} between DMF and

319   MeOH extracts (Table 2) was primarily ascribed to the fact that DMF can dissolve more

320   OC3 and OC4 than methanol (Table 1), but not the solvent effect.

321   *3.2 Collocated measurements and temporal variability*

322   Abs_{365} values of collocated Q_f and Q_b extracts in DMF are summarized in Table S5.

323   No significant difference was observed (Q_f $p = 0.96$; Q_b $p = 0.42$) between the two

324   samplers. After Q_b corrections, Abs_{365}, MAE_{365}, and Å of DMF extractable OC ($Abs_{365,d}$,

325    $MAE_{365,d}$, and $Å_d$) in $PM_{2.5}$ were calculated by averaging each pair of duplicate Q_f–Q_b

326   data, and are compared with those of methanol extracts ($Abs_{365,m}$, $MAE_{365,m}$, and $Å_m$)

327   in Table 3. Figure 1 shows comparisons between collocated measurements of $Abs_{365,d}$,

328    $MAE_{365,d}$, and $Å_d$. Generally, all comparisons indicated good agreement with COD <

329   0.20 (0.094–0.15). $Abs_{365,d}$ and $MAE_{365,d}$ had comparable uncertainty fractions (ARPD,

330   22.7% and 24.5%, Figure 1) as $Abs_{365,m}$ and $MAE_{365,m}$ (28.4% and 28.8%; Xie et al.,

331   2022). Since different primary combustion sources can have similar spectral

332   dependence for BrC absorption (Chen and Bond, 2010; Xie et al., 2017b; Xie et al.,

333   2018; Xie et al., 2019a), most $Å_d$ data clustered on the identity line with much lower

334   variability than $Abs_{365,d}$ and $MAE_{365,d}$. As shown in Table 3, average $Abs_{365,d}$ and

335    $MAE_{365,d}$ values were 30.7% ($p < 0.01$) and 17.3% ($p < 0.05$) larger than average

336    $Abs_{365,m}$ and $MAE_{365,m}$. Because the k value of BrC in bulk solution is directly estimated

337   from Abs_λ or MAE_λ (Liu et al., 2013; Liu et al., 2016; Lu et al., 2015), the estimation

338   method needs to be revised when ambient BrC is extracted using DMF instead of

339   MeOH. In comparison to $Å_m$ (6.81± 1.64; Table 3), the lower average $Å_d$ (5.25 ± 0.64,

340    $p < 0.01$) supports that more-absorbing BrC had less spectral dependence than less-

341   absorbing BrC.

342   Figure 2 compares the time series of Abs_{365}, MAE_{365}, and Å between the DMF and

343   MeOH extracts. Both DMF and MeOH extracts had significant ($p < 0.05$) higher

344   absorption at night-time than during the daytime due to the "photo-bleaching" effect

345   (Zhang et al., 2020; Xie et al., 2022). All the three parameters of DMF and MeOH

Atmospheric
Chemistry
and Physics
Discussions
Open Access
EGU

346   extracts exhibited consistency in winter (Figure 2) when biomass burning dominated

347   BrC absorption (Xie et al., 2022). While in later spring and summer (2019/05/15–

348   2019/08/01), average $Abs_{365,d}$ and $MAE_{365,d}$ values were more than two times greater

349   than the average $Abs_{365,m}$ and $MAE_{365,m}$. Many studies have identified a temporal

350   pattern of BrC absorption with winter maxima and summer minima based on

351   water/MeOH extraction methods (Lukács et al., 2007; Zhang et al., 2010; Du et al.,

352   2014; Zhu et al., 2018). Due to the low capability of water and MeOH in dissolving

353   large BrC molecules, BrC absorption and its temporal variations in these studies might

354   be biased. Moreover, the identification of BrC sources using receptor models is highly

355   dependent on the difference in the time series of input species (Dall'Osto et al., 2013).

356   Then, using DMF instead of MeOH for BrC extraction and measurements will lead to

357   distinct source apportionment results.

358   *3.3 Sources of DMF and MeOH Extractable BrC*

359   A final factor number of eight was determined based on the interpretability of

360   different base-case solutions (four to ten factors). Normalized factor profiles of seven-

361   to nine-factor solutions are compared in Figure S6. The seven-factor solution failed to

362   resolve the lubricating oil combustion factor characterized by hopanes and steranes

363   (Figure S6c). An unknown factor containing various source tracers related to crustal

364   dust (Ca^{2+} and Mg^{2+}), lubricating oil (hopanes and steranes), and soil microbiota (sugar

365   and sugar alcohols) was identified in the nine-factor solution (Figure S6i). Median and

366   mean values of input $Abs_{365,d}$, $Abs_{365,m}$ and bulk component concentrations agreed well

367   with PMF estimations (Table S6), and the strong correlations ($r = 0.86$–0.99) between

368   observations and PMF estimations indicated that the eight-factor solution simulated the

369   time series of input species well. In comparison to Xie et al. (2022), where Abs_{365} of

370   MeOH and water extracts were apportioned to nine sources using the same speciation

371   data, this work lumped secondary nitrate and sulfate to the same factor (termed

372   "secondary inorganics", Figure S6h), and the other seven factors had similar factor

373   profiles linked with biomass burning, non-combustion fossil, lubricating oil

374   combustion, coal combustion, dust resuspension, biogenic emission, and isoprene

375   oxidation. Interpretations of individual factors based on characteristic source tracers

376   and contribution time series were provided in previous work (Gou et al., 2021; Xie et

377   al., 2022). The average relative contributions of the identified factors to $Abs_{365,d}$,

378   $Abs_{365,m}$, and bulk components are listed in Table S7. Consistent contribution

379   distributions of $Abs_{365,m}$ were observed between Xie et al. (2022) and this study,

380   indicating that the PMF results were robust to the inclusion of $Abs_{365,d}$ data. Figure 3

381   compares the time series of factor contributions to $Abs_{365,d}$ and $Abs_{365,m}$. Although

382   $Abs_{365,d}$ and $Abs_{365,m}$ had comparable contributions from biomass burning, lubricating

383   oil combustion, and coal combustion (Figure 3a, c, d), other sources had significant (p

384   < 0.01) higher average contributions to $Abs_{365,d}$ than $Abs_{365,m}$.

385   The non-combustion fossil factor represents unburned fossil-fuel emissions (e.g.,

386   petroleum products), which contain substantial large organic molecules (e.g., high MW

387   PAHs; Simoneit and Fetzer, 1996; Mi et al., 2000). This might explain why the non-

388   combustion fossil factor contributed more $Abs_{365,d}$ than $Abs_{365,m}$ all over the year. Dust

389   resuspension and isoprene oxidation factors show prominent contributions to $Abs_{365,d}$

390   in spring and summer, respectively (Figure 3e, g). The dust resuspension factor had the

391   highest average contributions to both crustal materials (Ca^{2+} and Mg^{2+}) and

392   carbonaceous species (OC and EC; Table S7 and Figure S6), and was considered a

393   mixed source of crustal dust and motor vehicle emissions (Yu et al., 2020; Xie et al.,

394   2022). Besides the influences from primary emissions, aging processes of organic

395   components in dust aerosols can induce the formation of BrC through iron-catalyzed

396   polymerization (Link et al., 2020; Al-Abadleh, 2021; Chin et al., 2021). It was

397   demonstrated that the isoprene-derived polymerization products through aerosol-phase

398   reactions are light-absorbing chromophores (Lin et al., 2014; Nakayama et al., 2015).

399   The biogenic emission factor was characterized by tracers related to microbiota

400   activities (sugar and sugar alcohols) and decomposition of high plant materials (odd-

401   numbered alkanes) in soil (Rogge et al., 1993; Simoneit et al., 2004), and had negligible

402   contributions (< 0.1%) to $Abs_{365,d}$ and $Abs_{365,m}$. Evidence shows that secondary BrC

403   can be generated through gas-phase reactions of anthropogenic volatile organic

404   compounds with NO_X (Nakayama et al., 2010; Liu et al., 2016; Xie et al., 2017a),

405   aqueous reactions of SOA with reduced nitrogen-containing species (e.g., NH_4^+;

406   Updyke et al., 2012; Powelson et al., 2014; Lin et al., 2015), and evaporation of water

407   from droplets in the atmosphere containing soluble organics (Nguyen et al., 2012;

408   Kasthuriarachchi et al., 2020). Their contributions might be lumped into the secondary

409   inorganics factor due to the lack of OMMs. According to these results, one possible

410   explanation for the difference in time series between $Abs_{365,d}$ and $Abs_{365,m}$ (Figure 2) is

411   that large BrC molecules from unburned fossil fuels and atmospheric processes are less

412   soluble in MeOH than DMF.

413   **4 Conclusions and implications**

414   The comparisons of extraction efficiencies of ambient OC across selected solvents

415   and solvent mixtures reveal the necessity of replacing MeOH with DMF for measuring

416   BrC absorption in ambient aerosols, as low-volatile OC fractions containing strong

417   chromophores are less soluble in MeOH than DMF. The light-absorption measurements

418   of different solvent extracts show that DMF can extract more light-absorbing materials

419   from ambient aerosols than MeOH. Existing modeling studies on the radiative forcing

420   of BrC (Feng et al., 2013; Wang et al., 2014; Zhang et al., 2020) often retrieved or

421 estimated its optical properties from laboratory or ambient measurements based on

422 water/methanol extraction methods (Chen and Bond, 2010; Hecobian et al., 2010; Liu

423 et al., 2013; Zhang et al., 2013), and probably underestimated the contribution of BrC

424 to total aerosol absorption.

425 Although light-absorbing properties of DMF and MeOH extracts had good

426 agreement in cold periods, their distinct time series in spring and summer implies that

427 the contributions of certain BrC sources were underestimated or missed when the

428 MeOH extraction method was used. Source apportionment results of $Abs_{365,d}$ and

429 $Abs_{365,m}$ based on organic molecular marker data indicated that large and methanol

430 insoluble BrC molecules are likely coming from unburned fossil fuels and

431 polymerization of aerosol organics. Laboratory studies have observed the

432 polymerization process through heterogeneous reactions of several precursors (e.g.,

433 catechol; Lin et al., 2014; Link et al., 2020), but the structures and light-absorbing

434 properties of polymerization products in ambient aerosols are less understood and

435 warrant further study.

436

437 ***Data availability***

438 Data used in the writing of this paper is available at the Harvard Dataverse

439 (https://doi.org/10.7910/DVN/CGHPXB, Xu et al., 2022)

440

441 ***Author contributions***

442 MX designed the research. ZX, WF, YW, and HY performed laboratory experiments.

443 ZX, WF, and MX analyzed the data. ZX and MX wrote the paper with significant

444 contributions from YW and HL.

445

Atmospheric
Chemistry
and Physics
Discussions

452

References

454 Al-Abadleh, H. A.: Aging of atmospheric aerosols and the role of iron in catalyzing brown carbon
455   formation, Environ. Sci.: Atmos., 1, 297-345, 10.1039/D1EA00038A, 2021.
456 Atwi, K., Cheng, Z., El Hajj, O., Perrie, C., and Saleh, R.: A dominant contribution to light absorption
457   by methanol-insoluble brown carbon produced in the combustion of biomass fuels typically
458   consumed in wildland fires in the United States, Environ. Sci.: Atmos., 10.1039/D1EA00065A, 2022.
459 Bai, Z., Zhang, L., Cheng, Y., Zhang, W., Mao, J., Chen, H., Li, L., Wang, L., and Chen, J.:
460   Water/methanol-insoluble brown carbon can dominate aerosol-enhanced light absorption in port
461   cities, Environ. Sci. Technol., 54, 14889-14898, 10.1021/acs.est.0c03844, 2020.
462 Chen, Y., and Bond, T. C.: Light absorption by organic carbon from wood combustion, Atmos. Chem.
463   Phys., 10, 1773-1787, 10.5194/acp-10-1773-2010, 2010.
464 Cheng, Z., Atwi, K., Hajj, O. E., Ijeli, I., Fischer, D. A., Smith, G., and Saleh, R.: Discrepancies between
465   brown carbon light-absorption properties retrieved from online and offline measurements, Aerosol
466   Sci. Technol., 55, 92-103, 10.1080/02786826.2020.1820940, 2021.
467 Chin, H., Hopstock, K. S., Fleming, L. T., Nizkorodov, S. A., and Al-Abadleh, H. A.: Effect of aromatic
468   ring substituents on the ability of catechol to produce brown carbon in iron(iii)-catalyzed reactions,
469   Environ. Sci.: Atmos., 1, 64-78, 10.1039/D0EA00007H, 2021.
470 Dall'Osto, M., Querol, X., Amato, F., Karanasiou, A., Lucarelli, F., Nava, S., Calzolai, G., and Chiari,
471   M.: Hourly elemental concentrations in PM2.5 aerosols sampled simultaneously at urban
472   background and road site during SAPUSS – diurnal variations and PMF receptor modelling, Atmos.
473   Chem. Phys., 13, 4375-4392, 10.5194/acp-13-4375-2013, 2013.
474 Di Lorenzo, R. A., and Young, C. J.: Size separation method for absorption characterization in brown
475   carbon: Application to an aged biomass burning sample, Geophys. Res. Lett., 43, 458-465,
476   10.1002/2015gl066954, 2016.
477 Di Lorenzo, R. A., Washenfelder, R. A., Attwood, A. R., Guo, H., Xu, L., Ng, N. L., Weber, R. J.,
478   Baumann, K., Edgerton, E., and Young, C. J.: Molecular-size-separated brown carbon absorption for
479   biomass-burning aerosol at multiple field sites, Environ. Sci. Technol., 51, 3128-3137,
480   10.1021/acs.est.6b06160, 2017.
481 Du, Z., He, K., Cheng, Y., Duan, F., Ma, Y., Liu, J., Zhang, X., Zheng, M., and Weber, R.: A yearlong
482   study of water-soluble organic carbon in Beijing I: Sources and its primary vs. secondary nature,
483   Atmos. Environ., 92, 514-521, https://doi.org/10.1016/j.atmosenv.2014.04.060, 2014.
484 Feng, Y., Ramanathan, V., and Kotamarthi, V. R.: Brown carbon: a significant atmospheric absorber of
485   solar radiation? Atmos. Chem. Phys., 13, 8607-8621, 10.5194/acp-13-8607-2013, 2013.
486 Gou, Y., Qin, C., Liao, H., and Xie, M.: Measurements, gas/particle partitioning, and sources of nonpolar
487   organic molecular markers at a suburban site in the west Yangtze River Delta, China, J. Geophys.
488   Res. Atmos., 126, e2020JD034080, https://doi.org/10.1029/2020JD034080, 2021.
489 Hallar, A. G., Lowenthal, D. H., Clegg, S. L., Samburova, V., Taylor, N., Mazzoleni, L. R., Zielinska, B.
490   K., Kristensen, T. B., Chirokova, G., McCubbin, I. B., Dodson, C., and Collins, D.: Chemical and
491   hygroscopic properties of aerosol organics at Storm Peak Laboratory, J. Geophys. Res. Atmos., 118,
492   4767-4779, https://doi.org/10.1002/jgrd.50373, 2013.
493 Hecobian, A., Zhang, X., Zheng, M., Frank, N., Edgerton, E. S., and Weber, R. J.: Water-Soluble Organic

494   Aerosol material and the light-absorption characteristics of aqueous extracts measured over the
495   Southeastern United States, Atmos. Chem. Phys., 10, 5965-5977, 10.5194/acp-10-5965-2010, 2010.
496 Hems, R. F., Schnitzler, E. G., Liu-Kang, C., Cappa, C. D., and Abbatt, J. P. D.: Aging of atmospheric
497   brown carbon aerosol, ACS Earth Space Chem., 5, 722-748, 10.1021/acsearthspacechem.0c00346,
498   2021.
499 Huang, R.-J., Yang, L., Cao, J., Chen, Y., Chen, Q., Li, Y., Duan, J., Zhu, C., Dai, W., Wang, K., Lin, C.,
500   Ni, H., Corbin, J. C., Wu, Y., Zhang, R., Tie, X., Hoffmann, T., O'Dowd, C., and Dusek, U.: Brown
501   carbon aerosol in urban Xi'an, northwest China: The composition and light absorption properties,
502   Environ. Sci. Technol., 52, 6825-6833, 10.1021/acs.est.8b02386, 2018.
503 Huang, R.-J., Yang, L., Shen, J., Yuan, W., Gong, Y., Guo, J., Cao, W., Duan, J., Ni, H., Zhu, C., Dai, W.,
504   Li, Y., Chen, Y., Chen, Q., Wu, Y., Zhang, R., Dusek, U., O'Dowd, C., and Hoffmann, T.: Water-
505   insoluble organics dominate brown carbon in wintertime urban aerosol of China: Chemical
506   characteristics   and   optical   properties,   Environ.   Sci.   Technol.,   54,   7836-7847,
507   10.1021/acs.est.0c01149, 2020.
508 Hyslop, N. P., and White, W. H.: An evaluation of interagency monitoring of protected visual
509   environments (IMPROVE) collocated precision and uncertainty estimates, Atmos. Environ., 42,
510   2691-2705, https://doi.org/10.1016/j.atmosenv.2007.06.053, 2008.
511 Kasthuriarachchi, N. Y., Rivellini, L.-H., Chen, X., Li, Y. J., and Lee, A. K. Y.: Effect of relative humidity
512   on secondary brown carbon formation in aqueous droplets, Environ. Sci. Technol., 54, 13207-13216,
513   10.1021/acs.est.0c01239, 2020.
514 Kondo, Y., Miyazaki, Y., Takegawa, N., Miyakawa, T., Weber, R. J., Jimenez, J. L., Zhang, Q., and
515   Worsnop, D. R.: Oxygenated and water-soluble organic aerosols in Tokyo, J. Geophys. Res. Atmos.,
516   112, D01203, 10.1029/2006jd007056, 2007.
517 Lack, D. A., Langridge, J. M., Bahreini, R., Cappa, C. D., Middlebrook, A. M., and Schwarz, J. P.: Brown
518   carbon and internal mixing in biomass burning particles, Proc. Natl. Acad. Sci. U.S.A., 109, 14802-
519   14807, 10.1073/pnas.1206575109, 2012.
520 Laskin, A., Laskin, J., and Nizkorodov, S. A.: Chemistry of atmospheric brown carbon, Chem. Rev., 115,
521   4335-4382, 10.1021/cr5006167, 2015.
522 Li, X., Yang, Y., Liu, S., Zhao, Q., Wang, G., and Wang, Y.: Light absorption properties of brown carbon
523   (BrC) in autumn and winter in Beijing: Composition, formation and contribution of nitrated aromatic
524   compounds, Atmos. Environ., 223, 117289, https://doi.org/10.1016/j.atmosenv.2020.117289, 2020.
525 Li, Y., Ji, Y., Zhao, J., Wang, Y., Shi, Q., Peng, J., Wang, Y., Wang, C., Zhang, F., Wang, Y., Seinfeld, J.
526   H., and Zhang, R.: Unexpected oligomerization of small α-dicarbonyls for secondary organic aerosol
527   and brown carbon formation, Environ. Sci. Technol., 55, 4430-4439, 10.1021/acs.est.0c08066, 2021.
528 Lin, P., Laskin, J., Nizkorodov, S. A., and Laskin, A.: Revealing brown carbon chromophores produced
529   in reactions of methylglyoxal with ammonium sulfate, Environ. Sci. Technol., 49, 14257-14266,
530   10.1021/acs.est.5b03608, 2015.
531 Lin, P., Aiona, P. K., Li, Y., Shiraiwa, M., Laskin, J., Nizkorodov, S. A., and Laskin, A.: Molecular
532   characterization of brown carbon in biomass burning aerosol particles, Environ. Sci. Technol., 50,
533   11815-11824, 10.1021/acs.est.6b03024, 2016.
534 Lin, Y.-H., Budisulistiorini, S. H., Chu, K., Siejack, R. A., Zhang, H., Riva, M., Zhang, Z., Gold, A.,
535   Kautzman, K. E., and Surratt, J. D.: Light-absorbing oligomer formation in secondary organic
536   aerosol from reactive uptake of isoprene epoxydiols, Environ. Sci. Technol., 48, 12012-12021,
537   10.1021/es503142b, 2014.
538 Link, N., Removski, N., Yun, J., Fleming, L. T., Nizkorodov, S. A., Bertram, A. K., and Al-Abadleh, H.
539   A.: Dust-catalyzed oxidative polymerization of catechol and its impacts on ice nucleation efficiency
540   and optical properties, ACS Earth Space Chem., 4, 1127-1139, 10.1021/acsearthspacechem.0c00107,
541   2020.
542 Liu, J., Bergin, M., Guo, H., King, L., Kotra, N., Edgerton, E., and Weber, R. J.: Size-resolved
543   measurements of brown carbon in water and methanol extracts and estimates of their contribution to
544   ambient fine-particle light absorption, Atmos. Chem. Phys., 13, 12389-12404, 10.5194/acp-13-
545   12389-2013, 2013.
546 Liu, J., Lin, P., Laskin, A., Laskin, J., Kathmann, S. M., Wise, M., Caylor, R., Imholt, F., Selimovic, V.,
547   and Shilling, J. E.: Optical properties and aging of light-absorbing secondary organic aerosol, Atmos.
548   Chem. Phys., 16, 12815-12827, 10.5194/acp-16-12815-2016, 2016.
549 Lu, Z., Streets, D. G., Winijkul, E., Yan, F., Chen, Y., Bond, T. C., Feng, Y., Dubey, M. K., Liu, S., Pinto,
550   J. P., and Carmichael, G. R.: Light absorption properties and radiative effects of primary organic
551   aerosol emissions, Environ. Sci. Technol., 49, 4868-4877, 10.1021/acs.est.5b00211, 2015.
552 Lukács, H., Gelencsér, A., Hammer, S., Puxbaum, H., Pio, C., Legrand, M., Kasper-Giebl, A., Handler,

Atmospheric
Chemistry
and Physics
Discussions

553 M., Limbeck, A., Simpson, D., and Preunkert, S.: Seasonal trends and possible sources of brown
554 carbon based on 2-year aerosol measurements at six sites in Europe, J. Geophys. Res. Atmos., 112,
555 https://doi.org/10.1029/2006JD008151, 2007.

556 Mack, L. A., Levin, E. J. T., Kreidenweis, S. M., Obrist, D., Moosmüller, H., Lewis, K. A., Arnott, W. P.,
557 McMeeking, G. R., Sullivan, A. P., Wold, C. E., Hao, W. M., Collett Jr, J. L., and Malm, W. C.:
558 Optical closure experiments for biomass smoke aerosols, Atmos. Chem. Phys., 10, 9017-9026,
559 10.5194/acp-10-9017-2010, 2010.

560 Mi, H.-H., Lee, W.-J., Chen, C.-B., Yang, H.-H., and Wu, S.-J.: Effect of fuel aromatic content on PAH
561 emission from a heavy-duty diesel engine, Chemosphere, 41, 1783-1790,
562 https://doi.org/10.1016/S0045-6535(00)00043-6, 2000.

563 Nakayama, T., Matsumi, Y., Sato, K., Imamura, T., Yamazaki, A., and Uchiyama, A.: Laboratory studies
564 on optical properties of secondary organic aerosols generated during the photooxidation of toluene
565 and the ozonolysis of α-pinene, J. Geophys. Res. Atmos., 115, D24204, 10.1029/2010jd014387,
566 2010.

567 Nakayama, T., Sato, K., Tsuge, M., Imamura, T., and Matsumi, Y.: Complex refractive index of secondary
568 organic aerosol generated from isoprene/NOx photooxidation in the presence and absence of SO2,
569 J. Geophys. Res. Atmos., 120, 7777-7787, https://doi.org/10.1002/2015JD023522, 2015.

570 Nguyen, T. B., Lee, P. B., Updyke, K. M., Bones, D. L., Laskin, J., Laskin, A., and Nizkorodov, S. A.:
571 Formation of nitrogen- and sulfur-containing light-absorbing compounds accelerated by evaporation
572 of water from secondary organic aerosols, J. Geophys. Res. Atmos., 117, D01207,
573 10.1029/2011jd016944, 2012.

574 Powelson, M. H., Espelien, B. M., Hawkins, L. N., Galloway, M. M., and De Haan, D. O.: Brown carbon
575 formation by aqueous-phase carbonyl compound reactions with amines and ammonium sulfate,
576 Environ. Sci. Technol., 48, 985-993, 10.1021/es4038325, 2014.

577 Qin, C., Gou, Y., Wang, Y., Mao, Y., Liao, H., Wang, Q., and Xie, M.: Gas–particle partitioning of polyol
578 tracers at a suburban site in Nanjing, east China: increased partitioning to the particle phase, Atmos.
579 Chem. Phys., 21, 12141-12153, 10.5194/acp-21-12141-2021, 2021.

580 Rogge, W. F., Hildemann, L. M., Mazurek, M. A., Cass, G. R., and Simoneit, B. R. T.: Sources of fine
581 organic aerosol .4. Particulate abrasion products from leaf surfaces of urban plants, Environ. Sci.
582 Technol., 27, 2700-2711, 10.1021/es00049a008, 1993.

583 Saleh, R., Hennigan, C. J., McMeeking, G. R., Chuang, W. K., Robinson, E. S., Coe, H., Donahue, N.
584 M., and Robinson, A. L.: Absorptivity of brown carbon in fresh and photo-chemically aged biomass-
585 burning emissions, Atmos. Chem. Phys., 13, 7683-7693, 10.5194/acp-13-7683-2013, 2013.

586 Saleh, R., Robinson, E. S., Tkacik, D. S., Ahern, A. T., Liu, S., Aiken, A. C., Sullivan, R. C., Presto, A.
587 A., Dubey, M. K., Yokelson, R. J., Donahue, N. M., and Robinson, A. L.: Brownness of organics in
588 aerosols from biomass burning linked to their black carbon content, Nat. Geosci., 7, 647-650,
589 https://doi.org/10.1038/ngeo2220, 2014.

590 Saleh, R.: From measurements to models: Toward accurate representation of brown carbon in climate
591 calculations, Curr. Pollut. Rep., 6, 90-104, 10.1007/s40726-020-00139-3, 2020.

592 Schauer, J. J., Mader, B. T., Deminter, J. T., Heidemann, G., Bae, M. S., Seinfeld, J. H., Flagan, R. C.,
593 Cary, R. A., Smith, D., Huebert, B. J., Bertram, T., Howell, S., Kline, J. T., Quinn, P., Bates, T.,
594 Turpin, B., Lim, H. J., Yu, J. Z., Yang, H., and Keywood, M. D.: ACE-Asia intercomparison of a
595 thermal-optical method for the determination of particle-phase organic and elemental carbon,
596 Environ. Sci. Technol., 37, 993-1001, 10.1021/es020622f, 2003.

597 Shetty, N. J., Pandey, A., Baker, S., Hao, W. M., and Chakrabarty, R. K.: Measuring light absorption by
598 freshly emitted organic aerosols: Optical artifacts in traditional solvent-extraction-based methods,
599 Atmos. Chem. Phys., 19, 8817-8830, 10.5194/acp-19-8817-2019, 2019.

600 Simoneit, B. R. T., and Fetzer, J. C.: High molecular weight polycyclic aromatic hydrocarbons in
601 hydrothermal petroleums from the Gulf of California and Northeast Pacific Ocean, Org. Geochem.,
602 24, 1065-1077, https://doi.org/10.1016/S0146-6380(96)00081-2, 1996.

603 Simoneit, B. R. T., Elias, V. O., Kobayashi, M., Kawamura, K., Rushdi, A. I., Medeiros, P. M., Rogge,
604 W. F., and Didyk, B. M.: Sugars dominant water-soluble organic compounds in soils and
605 characterization as tracers in atmospheric particulate matter, Environ. Sci. Technol., 38, 5939-5949,
606 10.1021/es0403099, 2004.

607 Taylor, N. F., Collins, D. R., Lowenthal, D. H., McCubbin, I. B., Hallar, A. G., Samburova, V., Zielinska,
608 B., Kumar, N., and Mazzoleni, L. R.: Hygroscopic growth of water soluble organic carbon isolated
609 from atmospheric aerosol collected at US national parks and Storm Peak Laboratory, Atmos. Chem.
610 Phys., 17, 2555-2571, 10.5194/acp-17-2555-2017, 2017.

611 Updyke, K. M., Nguyen, T. B., and Nizkorodov, S. A.: Formation of brown carbon via reactions of

ammonia with secondary organic aerosols from biogenic and anthropogenic precursors, Atmos. Environ., 63, 22-31, https://doi.org/10.1016/j.atmosenv.2012.09.012, 2012.

Wang, X., Heald, C. L., Ridley, D. A., Schwarz, J. P., Spackman, J. R., Perring, A. E., Coe, H., Liu, D., and Clarke, A. D.: Exploiting simultaneous observational constraints on mass and absorption to estimate the global direct radiative forcing of black carbon and brown carbon, Atmos. Chem. Phys., 14, 10989-11010, 10.5194/acp-14-10989-2014, 2014.

Wang, X., Heald, C. L., Liu, J., Weber, R. J., Campuzano-Jost, P., Jimenez, J. L., Schwarz, J. P., and Perring, A. E.: Exploring the observational constraints on the simulation of brown carbon, Atmos. Chem. Phys., 18, 635-653, 10.5194/acp-18-635-2018, 2018.

Wang, Y., Hu, M., Wang, Y., Zheng, J., Shang, D., Yang, Y., Liu, Y., Li, X., Tang, R., Zhu, W., Du, Z., Wu, Y., Guo, S., Wu, Z., Lou, S., Hallquist, M., and Yu, J. Z.: The formation of nitro-aromatic compounds under high NOx and anthropogenic VOC conditions in urban Beijing, China, Atmos. Chem. Phys., 19, 7649-7665, 10.5194/acp-19-7649-2019, 2019.

Washenfelder, R. A., Attwood, A. R., Brock, C. A., Guo, H., Xu, L., Weber, R. J., Ng, N. L., Allen, H. M., Ayres, B. R., Baumann, K., Cohen, R. C., Draper, D. C., Duffey, K. C., Edgerton, E., Fry, J. L., Hu, W. W., Jimenez, J. L., Palm, B. B., Romer, P., Stone, E. A., Wooldridge, P. J., and Brown, S. S.: Biomass burning dominates brown carbon absorption in the rural southeastern United States, Geophys. Res. Lett., 42, 653-664, 10.1002/2014gl062444, 2015.

Weber, R. J., Sullivan, A. P., Peltier, R. E., Russell, A., Yan, B., Zheng, M., de Gouw, J., Warneke, C., Brock, C., Holloway, J. S., Atlas, E. L., and Edgerton, E.: A study of secondary organic aerosol formation in the anthropogenic-influenced southeastern United States, J. Geophys. Res. Atmos., 112, D13302, 10.1029/2007jd008408, 2007.

Xie, M., Chen, X., Hays, M. D., Lewandowski, M., Offenberg, J., Kleindienst, T. E., and Holder, A. L.: Light absorption of secondary organic aerosol: Composition and contribution of nitroaromatic compounds, Environ. Sci. Technol., 51, 11607-11616, 10.1021/acs.est.7b03263, 2017a.

Xie, M., Hays, M. D., and Holder, A. L.: Light-absorbing organic carbon from prescribed and laboratory biomass burning and gasoline vehicle emissions, Sci. Rep., 7, 7318, 10.1038/s41598-017-06981-8, 2017b.

Xie, M., Shen, G., Holder, A. L., Hays, M. D., and Jetter, J. J.: Light absorption of organic carbon emitted from burning wood, charcoal, and kerosene in household cookstoves, Environ. Pollut., 240, 60-67, https://doi.org/10.1016/j.envpol.2018.04.085, 2018.

Xie, M., Chen, X., Hays, M. D., and Holder, A. L.: Composition and light absorption of N-containing aromatic compounds in organic aerosols from laboratory biomass burning, Atmos. Chem. Phys., 19, 2899-2915, 10.5194/acp-19-2899-2019, 2019a.

Xie, M., Chen, X., Holder, A. L., Hays, M. D., Lewandowski, M., Offenberg, J. H., Kleindienst, T. E., Jaoui, M., and Hannigan, M. P.: Light absorption of organic carbon and its sources at a southeastern U.S. location in summer, Environ. Pollut., 244, 38-46, https://doi.org/10.1016/j.envpol.2018.09.125, 2019b.

Xie, M., Peng, X., Shang, Y., Yang, L., Zhang, Y., Wang, Y., and Liao, H.: Collocated Measurements of Light-absorbing organic carbon in PM2.5: Observation uncertainty and organic tracer-based source apportionment, J. Geophys. Res. Atmos., 127, e2021JD035874, https://doi.org/10.1029/2021JD035874, 2022.

Xu, Z., Feng, W., Wang, Y., Ye, H., Wang, Y., Liao, H., and Xie, M.: Replication Data for: Underestimation of brown carbon absorption based on the methanol extraction method and its impacts on source analysis, Harvard Dataverse, V1, https://doi.org/10.7910/DVN/CGHPXB, 2022.

Xu, L., Peng, Y., Ram, K., Zhang, Y., Bao, M., and Wei, J.: Investigation of the uncertainties of simulated optical properties of brown carbon at two Asian sites using a modified bulk aerosol optical scheme of the community atmospheric model version 5.3, J. Geophys. Res. Atmos., 126, e2020JD033942, https://doi.org/10.1029/2020JD033942, 2021.

Yan, F., Kang, S., Sillanpää, M., Hu, Z., Gao, S., Chen, P., Gautam, S., Reinikainen, S.-P., and Li, C.: A new method for extraction of methanol-soluble brown carbon: Implications for investigation of its light absorption ability, Environ. Pollut., 262, 114300, https://doi.org/10.1016/j.envpol.2020.114300, 2020.

Yang, L., Shang, Y., Hannigan, M. P., Zhu, R., Wang, Q. g., Qin, C., and Xie, M.: Collocated speciation of PM2.5 using tandem quartz filters in northern nanjing, China: Sampling artifacts and measurement uncertainty, Atmos. Environ., 246, 118066, https://doi.org/10.1016/j.atmosenv.2020.118066, 2021.

Yu, Y., Ding, F., Mu, Y., Xie, M., and Wang, Q. g.: High time-resolved PM2.5 composition and sources at an urban site in Yangtze River Delta, China after the implementation of the APPCAP,

671   Chemosphere, 261, 127746, https://doi.org/10.1016/j.chemosphere.2020.127746, 2020.

672   Zhang, A., Wang, Y., Zhang, Y., Weber, R. J., Song, Y., Ke, Z., and Zou, Y.: Modeling the global radiative
673   effect of brown carbon: a potentially larger heating source in the tropical free troposphere than black
674   carbon, Atmos. Chem. Phys., 20, 1901-1920, 10.5194/acp-20-1901-2020, 2020.

675   Zhang, X., Hecobian, A., Zheng, M., Frank, N. H., and Weber, R. J.: Biomass burning impact on PM2.5
676   over the southeastern US during 2007: integrating chemically speciated FRM filter measurements,
677   MODIS fire counts and PMF analysis, Atmos. Chem. Phys., 10, 6839-6853, 10.5194/acp-10-6839-
678   2010, 2010.

679   Zhang, X., Lin, Y.-H., Surratt, J. D., and Weber, R. J.: Sources, composition and absorption Ångström
680   exponent of light-absorbing organic components in aerosol extracts from the Los Angeles basin,
681   Environ. Sci. Technol., 47, 3685-3693, 10.1021/es305047b, 2013.

682   Zhu, C.-S., Cao, J.-J., Huang, R.-J., Shen, Z.-X., Wang, Q.-Y., and Zhang, N.-N.: Light absorption
683   properties of brown carbon over the southeastern Tibetan Plateau, Sci. Total Environ., 625, 246-251,
684   https://doi.org/10.1016/j.scitotenv.2017.12.183, 2018.

Table 1. SEOC concentrations and extraction efficiencies (η, %) of total OC and OC fractions for different solvents.

	OC prior to extractions	Water[a]	MeOH[b]	MeOH/DCM (1:1)[b]	MeOH/DCM (1:2)[b]	THF[b]	DMF[a]
One-time extraction (N = 11)							
SEOC, µg m⁻³							
Total OC	9.36 ± 2.27	6.38 ± 2.03	7.85 ± 2.40	7.08 ± 1.32	6.99 ± 1.71	6.14 ± 2.01	8.49 ± 2.52
OC1	0.66 ± 0.21	0.61 ± 0.20	0.64 ± 0.21	0.65 ± 0.20	0.64 ± 0.22	0.59 ± 0.18	0.59 ± 0.24
OC2	2.69 ± 0.55	2.20 ± 0.60	2.50 ± 0.55	2.34 ± 0.41	2.37 ± 0.46	2.09 ± 0.55	2.48 ± 0.60
OC3	3.35 ± 0.93	1.82 ± 0.80	2.48 ± 0.96	2.23 ± 0.49	2.18 ± 0.70	1.98 ± 0.93	2.86 ± 1.01
OC4	2.75 ± 0.81	1.76 ± 0.65	2.23 ± 0.84	1.86 ± 0.51	1.78 ± 0.61	1.48 ± 0.61	2.56 ± 0.87
η (%)							
Total OC		66.7 ± 8.58	82.3 ± 8.68	76.0 ± 7.70	74.3 ± 7.83	64.2 ± 8.08	89.0 ± 7.96
OC1		91.7 ± 4.85	96.1 ± 6.73	97.9 ± 5.02	97.4 ± 4.35	89.6 ± 9.55	88.8 ± 4.98
OC2		80.8 ± 8.11	92.7 ± 3.69	87.7 ± 5.87	88.5 ± 7.21	76.9 ± 7.62	91.4 ± 6.17
OC3		52.4 ± 11.8	73.0 ± 11.5	68.1 ± 8.64	65.2 ± 10.2	57.6 ± 12.0	84.3 ± 9.79
OC4		63.3 ± 9.13	80.3 ± 11.4	69.0 ± 9.26	64.5 ± 8.11	52.7 ± 5.86	92.8 ± 9.69
Two-time extraction (N = 10)							
SEOC, µg m⁻³							
Total OC	10.9 ± 4.93	7.74 ± 4.01	9.33 ± 4.11	9.34 ± 4.19	9.11 ± 4.04	7.56 ± 3.38	10.4 ± 4.80
OC1	0.66 ± 0.47	0.62 ± 0.45	0.62 ± 0.49	0.59 ± 0.50	0.60 ± 0.51	0.59 ± 0.49	0.60 ± 0.47
OC2	2.76 ± 0.77	2.20 ± 0.59	2.60 ± 0.66	2.57 ± 0.65	2.60 ± 0.68	2.28 ± 0.53	2.69 ± 0.78
OC3	4.11 ± 2.01	2.55 ± 1.62	3.26 ± 1.62	3.37 ± 1.68	3.20 ± 1.58	2.62 ± 1.39	3.88 ± 1.95
OC4	3.36 ± 1.77	2.38 ± 1.42	2.84 ± 1.42	2.81 ± 1.47	2.71 ± 1.39	2.08 ± 1.06	3.23 ± 1.70
η (%)							
Total OC		69.9 ± 5.88	86.6 ± 7.86	86.2 ± 8.73	84.8 ± 7.76	70.1 ± 8.01	95.6 ± 3.67
OC1		93.6 ± 4.08	90.3 ± 13.9	82.6 ± 25.9	83.8 ± 22.4	82.9 ± 15.1	92.2 ± 13.9
OC2		80.1 ± 5.01	94.8 ± 4.20	93.6 ± 4.94	94.7 ± 2.51	83.5 ± 6.86	97.2 ± 2.12
OC3		59.0 ± 10.6	80.0 ± 10.2	82.3 ± 9.86	79.1 ± 10.6	63.9 ± 10.7	94.2 ± 4.15
OC4		69.3 ± 6.46	86.3 ± 12.0	84.3 ± 12.0	82.7 ± 13.3	62.9 ± 7.76	96.9 ± 5.18

[a] Concentrations of rOC in extracted filters were measured after the baking process (100 °C, 2 h); [b] rOC was measured when extracted filters were air dried.

Table 2. Light-absorbing properties of SEOC following one-time and two-time extraction procedures.

Solvent	Water	MeOH	MeOH/DCM (1:1)	MeOH/DCM (1:2)	THF	DMF
One-time extraction						
Abs_{365}, Mm^{-1}	5.13 ± 2.04	11.9 ± 5.83	10.3 ± 4.42	8.12 ± 3.38	5.48 ± 3.01	17.5 ± 8.05
Abs_{550}, Mm^{-1}	0.35 ± 0.12	1.28 ± 0.87	0.97 ± 0.55	0.35 ± 0.47	0.42 ± 0.47	4.40 ± 2.34
MAE_{365}, $m^2\,g^{-1}$ C	0.87 ± 0.19	1.46 ± 0.41	1.41 ± 0.36	1.13 ± 0.22	0.87 ± 0.25	2.02 ± 0.58
MAE_{550}, $m^2\,g^{-1}$ C	0.062 ± 0.028	0.15 ± 0.084	0.13 ± 0.054	0.042 ± 0.52	0.059 ± 0.56	0.30 ± 0.12
Å	6.63 ± 0.49	5.44 ± 0.75	5.65 ± 0.54	6.59 ± 0.66	6.17 ± 0.69	4.52 ± 0.41
Two-time extraction						
$Abs_{365,1st}$,[a] Mm^{-1}	6.64 ± 4.25	14.1 ± 7.09	14.6 ± 8.05	11.6 ± 6.78	7.17 ± 4.26	20.5 ± 10.6
$Abs_{550,1st}$,[a] Mm^{-1}	0.42 ± 0.12	1.34 ± 0.70	1.34 ± 0.83	0.84 ± 0.50	0.53 ± 0.27	2.82 ± 1.44
Abs_{365},[b] Mm^{-1}	8.26 ± 5.21	15.5 ± 7.76	16.8 ± 8.82	14.0 ± 8.91	8.35 ± 4.81	21.9 ± 11.2
Abs_{550},[b] Mm^{-1}	0.50 ± 0.18	1.60 ± 0.78	1.64 ± 0.99	1.22 ± 0.98	0.69 ± 0.43	3.01 ± 1.49
MAE_{365}, $m^2\,g^{-1}$ C	1.19 ± 0.26	1.70 ± 0.60	1.80 ± 0.52	1.50 ± 0.51	1.10 ± 0.40	2.11 ± 0.49
MAE_{550}, $m^2\,g^{-1}$ C	0.082 ± 0.30	0.19 ± 0.11	0.17 ± 0.083	0.13 ± 0.069	0.094 ± 0.054	0.29 ± 0.075
Å	6.32 ± 0.58	5.37 ± 0.57	5.47 ± 0.67	5.57 ± 0.39	6.06 ± 0.54	4.53 ± 0.21

[a] Light absorption coefficient of SEOC after the first extraction; [b] sum of SEOC absorption in 1st and 2nd extracts.

Table 3. Comparisons of light-absorbing properties of ambient $PM_{2.5}$ extracts in DMF and MeOH derived from duplicate Q_f–Q_b data ($N = 109$).

	DMF			MeOH[a]		
	Median	Mean ± std	Range	Median	Mean ± std	Range
Abs_{365}, Mm-1	6.99	8.42 ± 5.40	1.14–30.8	5.59	6.43 ± 4.66	0.38–29.6
MAE_{365}, m^2 $g^{-1}C$	1.13	1.20 ± 0.49	0.34–2.45	0.91	1.03 ± 0.58	0.089–2.49
Å	5.21	5.25 ± 0.64	3.21–6.82	6.49	6.81 ± 1.64	4.34–11.3

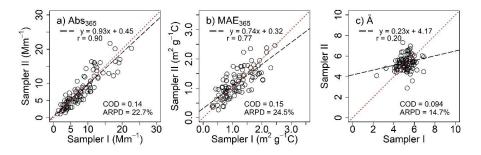[a] Data for MeOH extracts were obtained from Xie et al. (2022).

Figure 1

Figure 1. Comparisons between collocated measurements for light-absorbing properties of $PM_{2.5}$ extracts in DMF after Q_b corrections.
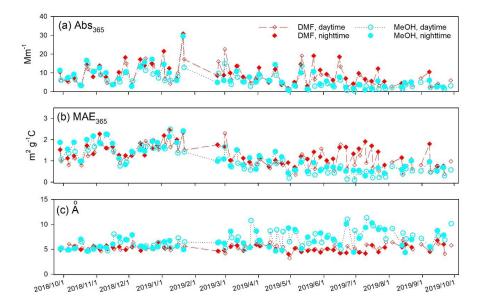
Figure 2

Figure 2. Time series comparisons of light-absorbing properties of DMF and MeOH extracts using artifact-corrected data. MeOH extract data were obtained from Xie et al. (2022).
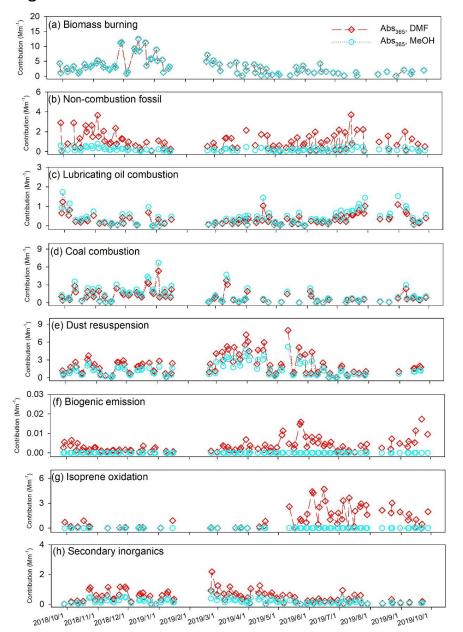
Figure 3

Figure 3. Time series of factor contributions to Abs$_{365}$ of DMF and MeOH extracts of ambient PM$_{2.5}$ samples.